High quality electron bunches for a multistage GeV accelerator with resonant multipulse ionization injection

Paolo Tomassini,[1,*] Davide Terzani,[1] Luca Labate,[1,2] Guido Toci,[3] Antoine Chance,[4] Phu Anh Phi Nghiem,[4] and Leonida A. Gizzi[1,2]

[1]*Intense Laser Irradiation Laboratory, INO-CNR, Via Moruzzi 1, 56124 Pisa, Italy*
[2]*INFN, Sect. of Pisa, Largo Bruno Pontecorvo 3, 56127 Pisa, Italy*
[3]*INO-CNR, Largo Enrico Fermi 2, 56125 Firenze, Italy*
[4]*CEA-Irfu, Centre de Saclay, Université Paris-Saclay, 91191 Gif sur Yvette, France*

(Received 19 July 2019; published 12 November 2019)

Laser wakefield acceleration of GeV electrons is becoming a mature technique, so that a reliable accelerator delivering stable beams to users communities can now be considered. In such a context, two plasma stages, one injector and one booster stage, offer a flexible solution for optimization. For the injector we consider here the resonant multipulse ionization injection (ReMPI) that can be optimized to generate electron bunches with high enough quality to be efficiently transported to the second stage. In order to better control the beam-loading effect and optimize the beam manipulation after the plasma downramp, a quasiround beam is preferable. In this respect, we present analytical and particle-in-cell results concerning the tunnel-ionization process in presence of two, orthogonally polarized, laser pulses with different wavelengths. We also show, by means of hybrid fluid/PIC numerical simulations, that a stable working point with the ReMPI injector exists at 32 pC, 4 kA peak current, with mean energy of 150 MeV, energy spread of 1.65% *rms*, normalized emittance $\epsilon_n = 0.23$ μm and divergence of 0.6 mrad. The scheme relies on a 150 TW Ti:Sa laser modified to achieve a four-pulses driver train and a third harmonics ionization pulse.

DOI: 10.1103/PhysRevAccelBeams.22.111302

I. INTRODUCTION

Advanced acceleration techniques are being pursued via different approaches, aiming at compact, more affordable systems to drive secondary radiation sources [1–10] or even future particle colliders [11–13]. In this context, laser wakefield acceleration (LWFA) of electrons offers a very promising path, with experiments showing further increase of maximum energy, now approaching 8 GeV [14], including staging exploration [15–19] and high repetition rate operation at the lower energy end [20]. In view of the construction of the first user facility based on plasma acceleration, effort is now directed toward the demonstration of stable operation of a GeV scale electron beam at high specification, as those needed for an x-ray free electron laser (FEL) in the EuPRAXIA project [21].

A two-stage configuration was conceived and developed to this purpose and is now optimized to meet required electron beam performances. It is composed by a 150 MeV injector based on the resonant multipulse ionization injection (ReMPI) [22] and a 5 GeV booster, linked by a magnetic transfer line. The booster has been thoroughly optimized and it is proven that the above requested final beam parameters can be achieved, at the condition that beam quality at the booster entrance is large enough [23].

The injector module should operate in a 10–100 Hz repetition rate configuration, delivering good beam-quality bunches with a stable phase-space quality set. Such a beam-quality refers mainly on the beam charge ($Q > 30$ pC), on the relative energy spread ($\sigma_E/E \ll 5\%$), on the transverse normalized emittance ($\epsilon_n \ll 1$ μmrad) and, finally, on the mean divergence angle $\sigma_\theta \ll 1$ mrad).

The beam-quality request at the injector exit is twofold. First, FEL lasing at the final energy of 5 GeV fixes an upper value of the final normalized emittance of about 1 μmrad [24]. In EuPRAXIA, a standard transfer beamline between each LWFA stage is envisaged, as the promising schemes based on matched longitudinally-tailored plasma modules [25,26] needs a dedicated study to be adapted in our resonant-excitation regime. In standard transfer beamlines, however, a severe emittance growth due to chromatic effects can spoil out transverse quality [27,28]. Our simulations (not shown here) show that in the present configuration an increase of the normalized emittance of about a factor two will occur between the

*paolo.tomassini@ino.it

injector module and the booster, provided that the energy spread at the injector exit is below 5% *rms*. Therefore, the final constraints on the emittance and the energy spread at the end of the injector read $\epsilon_n < 0.5$ mm mrad, $\sigma_E/E \ll 5\%$

Second, in the transfer line the increase in normalized emittance due to chromatic effects can be drastically reduced provided that the beam divergence at the injector exit is made low enough, i.e., the Twiss γ factor of the beam is as low as possible. From beam transport simulations we can infer that a Twiss $\gamma = \sigma(x')^2/\epsilon < 200$ m^{-1} is low enough to limit the normalized emittance increase down 100% (here x is the transverse position, $x' \equiv dx/ds$ where s is the longitudinal position of the beam center and $\epsilon = \sqrt{\langle x^2\rangle\langle x'^2\rangle - \langle xx'\rangle^2}$ is the *rms* trace emittance). In addition to the beam-quality parameters mentioned above, additional constraints arise from FEL lasing threshold and saturation power: a beam charge of at least 30 pC with duration not exceeding 10 fs must be assured, too. This induces a peak current of about 3 kA, which is beneficial for reducing the undulator length and for enhancing the source brilliance [24]. Table I summarizes the whole set of beam-quality requirements that, we stress here, the bunch *must comply at the same time*.

Since the set of constraints is very demanding to fulfill as a whole, we need a particle injection scheme capable of generating very low emittance bunches with a selectable and stable amount of charge, with tunable bunch duration and possibly driven by a single standard 100-TW class Ti:Sa laser system. Many injections schemes can produce low-emittance bunches. Controlled wave-breaking by density downramp [29–34] can generate normalized emittances of about 0.2 μmrad [31], and density downramp injection in the blow-out regime [35] is capable of generating beams with brightness exceeding 10^{20} A/m^2/rad^2. Two-color ionization injection [36] is extremely flexible and capable of generating normalized emittances of the order of tens of nmrad. The two-color ionization scheme needs the use of two laser systems: the "driver" pulse excites the plasma wave and is delivered by a long-wavelength (e.g., CO_2) system, while a synchronized pulse (the "ionization" pulse) from a Ti:Sa system extracts the electrons from the dopant. To date, however, long-wavelength ($\lambda > 5$ μm), high-power ($P > 100$ TW) and ultrashort ($T \ll 100$ fs) laser systems are lacking and hopefully will be available in a short future.

TABLE I. Requested beam quality ("R" raw) and quality parameters obtained by means of the simulations reported in the paper ("O" raw). The relative energy spread $\sigma(E)/E$, normalized emittance ϵ_n, Twiss parameter γ, charge Q and peak current I are shown.

	$\sigma(E)/E$	ϵ_n	Twiss γ	Q	I
R	$\ll$5%	$\ll$1 μmrad	$<$200 m^{-1}	$\geq$30 pC	$>$1 kA
O	1.65%	0.23 μmrad	140 m^{-1}	32 pC	4 kA

To implement a flexible and stable injection scheme capable of generating low-emittance bunches, we have proposed a technique that only makes use of a single 100-TW class Ti:Sa laser system. In the resonant multipulse ionization injection [22,37,38] scheme, the CO_2 driver is substituted by a train of pulses that excites the large amplitude wakefield through the multipulse LWFA mechanism [39–42] [see Fig. 1(a)], keeping each pulse electric field under the ionization threshold for the selected dopant. Subsequently, a tightly focused, low amplitude, pulse in second/third harmonics in the tail of the train ionizes the dopant (e.g., Nitrogen or Argon) injecting the electrons into the wakefield with an ultralow emittance. The intensity of the pulses in the driving train must be chosen so as the plasma wave amplitude is large enough to trap the newborn electrons. As a result, the electrons are extracted close to the axis by the ionizing pulse, they quiver with a very low transverse momentum and are trapped in the focusing region of the same bucket, thus constituting a low-emittance bunch. To produce such a configuration, a single Ti:Sa pulse can be time shaped to form the driver train of pulses, while a small portion of the same pulse can be frequency doubled/tripled and then delivered with a tight focusing for the ionization process [see Figs. 1(a),(b)].

In any ionization injection scheme (as two-color and ReMPI, but also on standard low-quality schemes [43]) and with the notable exception of the transverse-colliding pulses [44], electron bunches shapes strongly deviate from axial symmetry, thus making transverse evolution nontrivial when a severe beam-loading is present. Also, their manipulation with some standard beam optics or plasma lenses result cumbersome. The usage of a circularly polarized pulse instead of a linearly polarized one would produce an axially symmetrical bunch, of course, but in that case the transverse emittance would increase dramatically. In order to comply with both a quasiround beam matched beam and low-emittance requirements, we analyzed the opportunity of a partial overlapping between the ionizing pulse and the orthogonally polarized driving train, as naturally arises in an optimized configuration. Analytical results and PIC simulations helped us in defining a working point showing an excellent axial symmetry of the electron beam, starting from the early stages if its injection up to its extraction from the plasma.

The paper is organized as follows. In Sec. II the ReMPI scheme and the new quasiround beam option are described in details, along with the set of parameters chosen for the selected working point. In Sec. III the stability study of the beam-quality vs laser/target imperfections is reported, showing that such a working point is stable against spatial and temporal jitters. Section IV is finally devoted to a discussion of the numerical and analytical results presented in the paper.

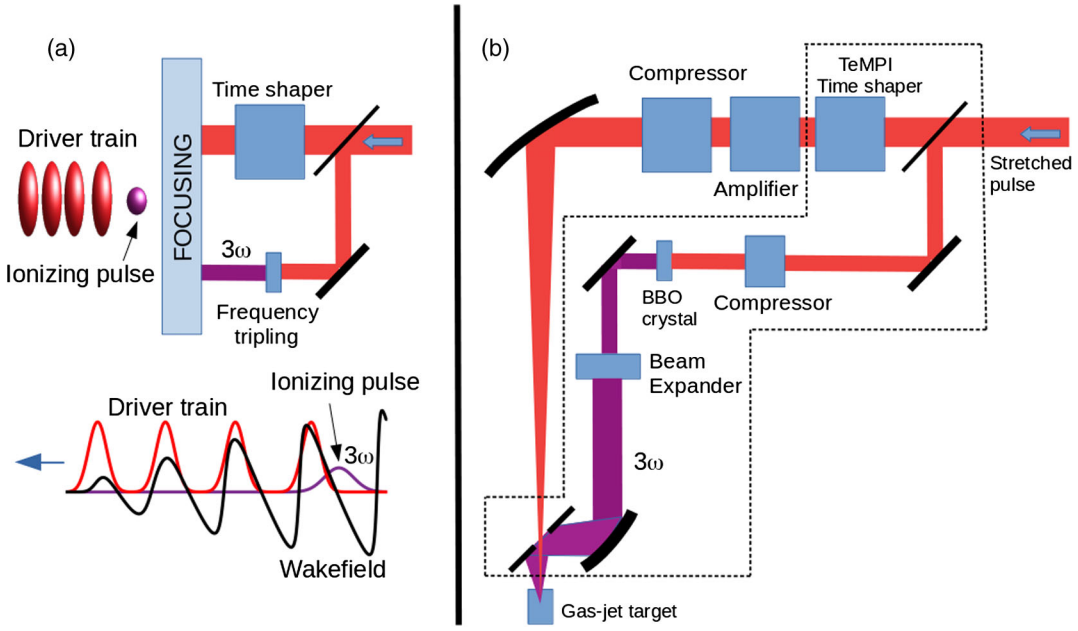

FIG. 1. The ReMPI setup. (a) Conceptual scheme: the incoming pulse passes through a beam-splitter; a portion (top line) is time shaped as a train of pulses, while a smaller portion is frequency tripled and tightly focused in the rear of the train. The driver train (four pulses, red line) resonantly excites an high-amplitude plasma wave (black line) and the ionizing pulse (perpendicular polarization, purple) is approximately placed in the node of the wakefield. (b) Experimental setup: the stretched pulse passes through a beam-splitter. The most energetic portion is time shaped through the passage into a TeMPI time-splitter (see text), further amplified and re-compressed by the grating compressor. The diver train is finally focused on the target (a gas-jet, gas-cell or a capillary delivering a mixture of H/He and a dopant (N, Ar), thus exciting a large-amplitude plasma wave. The low-energy portion of the initial pulse is amplified, frequency tripled through the passage into a thin nonlinear BBO crystal, temporally recompressed and radially magnified by using a reflective-beam expander. The 3ω ionizing pulse is finally tightly focused with a short parabola and made collinear with the driver train by using an holed mirror. The region inside the dashed lines constitutes the experimental apparatus needed in addition to a standard LWFA setup.

II. THE WORKING POINT FOR THE RESONANT MULTIPULSE IONIZATION INJECTION

A. The choice of the number of pulses in the driving train

Since the main goal of the ReMPI scheme is the production of an high-quality accelerated bunch, we have to properly match the choice of the dopant, of the number of pulses in the driving train and of the ionizing pulse amplitude, in order to fulfill the request on the admissible maximum value for the emittance. To select a proper dopant, we recall analytical results and simulations in Ref. [45], which show that the minimum normalized emittance achievable by using a linearly polarized pulse can be as low as

$$\epsilon_{n,\min} \simeq \frac{1}{\sqrt{2}} w_{0,\mathrm{ion}} \cdot a_{0,\mathrm{ion}} \cdot \Delta^2 = \frac{1}{\sqrt{2}} w_{0,\mathrm{ion}} \cdot a_{0,\mathrm{ion}}^2 / a_c, \quad (1)$$

being $\Delta \equiv \sqrt{a_{0,\mathrm{ion}}/a_c}$, $a_c = 0.108 \cdot \lambda_{\mathrm{ion}} (U_i/U_H)^{3/2}$ (see Eq. (26) in [45] and (4) in [22]). Here $a_{0,\mathrm{ion}}$, $w_{0,\mathrm{ion}}$, and λ_{ion} represent the ionization pulse normalized peak amplitude $a = eA/mc^2$, waist size and wavelength in microns, respectively, and U_i, U_H are the ionization energies for the selected atom state and of the Hydrogen ground state ($U_H \simeq 13.6$ eV). If the transition $Ar^{8+} \rightarrow Ar^{9+}$ is selected, along with an ionization pulse in third harmonics with minimum waist $w_{0,\mathrm{ion}} = 4$ μm and normalized amplitude $a_{0,\mathrm{ion}} = 0.31$ so as to extract a few tens of pC of charge, we derive from Eq. (1) a minimum emittance $\epsilon_{n,\min} \simeq 50$ nmrad. On the other hand, by using the transition $N^{5+} \rightarrow N^{6+}$ and a similar third harmonics pulse with amplitude $a_{0,\mathrm{ion}} = 0.63$, the minimum achievable emittance can be estimated as $\epsilon_{n,\min} \simeq 150$ nmrad.

The electrons extracted by tunnel field-ionization must be trapped by the plasma wave having pulsation ω_p and phase velocity $\beta_{\mathrm{ph}} \simeq (1 - \omega_p^2/2\omega_0^2)$. To minimize the final energy spread, it is preferable that the electrons reach β_{ph} when they are in the vicinity of the accelerating field peak. Such a "strong trapping" condition (see Eq. (3) in [22]) should be therefore satisfied by the plasma wave, whose amplitude E_z needs to comply with

$$E_{\mathrm{norm}}^2/2 + \beta_{\mathrm{ph}} \sqrt{(1 + E_{\mathrm{norm}}^2/2)^2 - 1} = 1 - 1/\gamma_{\mathrm{ph}}, \quad (2)$$

where $E_{\mathrm{norm}} \equiv \max(E_z)/E_0$ is the peak longitudinal electric field normalized to the nonrelativistic wavebreaking limit $E_0 = mc\omega_p/e$. For plasma densities typically implied in

LWFA, e.g., 10^{17} cm$^{-3} \lesssim n_e \lesssim 10^{19}$ cm^{-3}, Lorentz factor relative to the wave phase velocity $\gamma_{\rm ph} \simeq \omega_0/\omega_p \gg 1$, so that Eq. (2) simplifies to $E_{\rm norm}^2/2 + \sqrt{(1+E_{\rm norm}^2/2)^2 - 1} \simeq 1$, and the requested amplitude is $E_{\rm norm} \simeq 0.7$ *independently on the chosen density.* With the constraint of leaving each pulse in the driving train with amplitude below the saturation threshold (which is a fixed number once the dopant species has been selected), the requested plasma wave amplitude is obtained by increasing the number of pulses that resonantly excite the wave. As a final result, the minimum number of pulses to reach a plasma wave normalized amplitude $E_{\rm norm} \simeq 0.7$ is just a function of the dopant species (see also Fig. 3 in [22]). As it has been evaluated earlier, if we need to limit the minimum achievable emittance to $\epsilon_{n,\rm min} \lesssim 50$ nmrad, Argon could be selected as dopant and a minimum number of six pulses should be used (a number of eight pulses is a better choice). In the case of acceptable normalized emittance of about 150 nm rad, a simpler option with two/four pulses in the train can be employed.

As from Table I ("R") we are not forced to limit the normalized emittance below 150 nm rad, the simpler option that uses a four-pulses driver train and Nitrogen as dopant has been selected. The optimization process led to the excitation of a nonlinear wave with amplitude $\max(E_z) \simeq 0.9E_0$, i.e., slightly above the strong-trapping condition, with a train of four pulses obtained with a 150 TW Ti:Sa laser system.

B. The pulse train generation scheme

Over the past few years, a few optical schemes were proposed in order to generate a train of ultrashort pulses from a CPA Ti:Sa chain [42,46,47]. While the method employed in [42] does not comply with the requirement of the ReMPI scheme to have small differences among the intensity of each pulse in the train, the methods proposed in [46,47] can provide pulse trains with a nearly constant pulse intensity along the train. However, none of them can be considered as a viable method to be used when an injector has to be operated, as in the EuPRAXIA case envisaged here, at a relatively high repetition rate (10–100 Hz). Indeed, both these schemes involve a ~50% energy waste, which turns out to be unfeasible, ultimately due to the issues related to the thermal management arising in Ti:Sa CPA architectures. In order to investigate a viable option for high energy/power and high rep rate systems, such as those currently under conceptual design for the EuPRAXIA project, we studied an optical scheme derived from the one proposed in [47]. The concept described there is based upon the usage of birefringent plates of increasing thicknesses and crossed polarizations, which produce delayed replicas of the original pulse, and linear polarizers. In contrast to the arrangement described there, in our scheme such a stack is used, on the stretched pulse, early (i.e., upstream) in the CPA amplification chain, so that the energy loss intrinsic to the optical scheme can be recovered at a relatively small price in terms of additional pump energy.

A thorough description and discussion of such an optical scheme is beyond the scope of this paper and will be reported elsewhere. Here we only mention that numerical simulations of the entire amplification chain of the laser currently being considered for the EuPRAXIA injector [48] have been carried out using the code MIRO [49], in view of the fact that both interference and nonlinear effects occurring with this multiplexing scheme may lead to potentially harmful intensity enhancement along the chain. While these effects have been seen to be manageable in our envisioned laser design, for the sake of the present work it is worth to note the appearance of spurious pulses with respect to the ideal train pulse. The time profile of the laser train intensity, as an output of a MIRO simulation with a 150 TW Ti:Sa laser system and pulse-to-pulse delay of about 100 fs, is shown in Fig. 2. As it is clear form the figure, the actual train features some pre-and post-pulses with lower amplitude with respect to the four main pulses. However, while prepulses efficiently do excite the plasma wave, the postpulses do it in the buckets *behind* the bunch, so the overall (usable) energy conversion is less than (but close to) 100%.

Moreover, just after each of the four pulses, lower intensity peaks are visible. These peaks are caused mainly by self-phase modulation effects on the pulse. Nonetheless these satellite pulses do not interfere with the wake excitation, due to their low intensity and short duration.

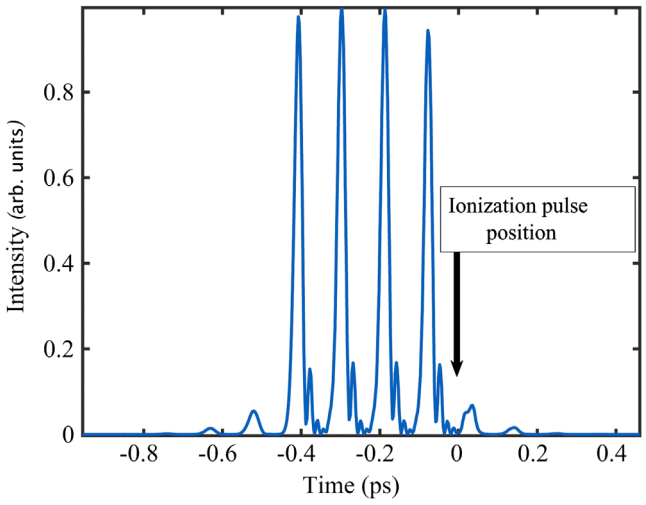

FIG. 2. The intensity profile of the train of 30 fs long pulses generated with the TEMPI technique. The train moves through the left. The pulse-to-pulse delay is close to the resonant plasma period. Note the presence of low intensity prepulses and post-pulses due to imperfections in pulse(s) compression. The high intensity pulses possess a structured train of low intensity ripples (of about 20% of the peak intensity) caused by nonlinear effects during the pulses amplification.

C. The driving train and ionization pulse working points

The longitudinal profile of the driver train has been obtained with dedicated MIRO simulations, by assuming 30 fs long pulses and pulse-to-pulse delay of about 100 fs, which has been tuned so as to excite a plasma wave with background density on $n_e = 1.1 \times 10^{18}$ cm^{-3}. The 150 TW pulse from a state-of-the-art Ti:Sa laser system is decomposed in a train of pulses delivering an overall energy of 4.5 J in 28 fs (see Fig. 2), with a conversion efficiency of about 90%.

The train is focused with a $F/20$ off-axis parabola down to a spot of minimum waist $w_0 = 27.5$ μm, with a peak intensity of 2.5×10^{18} W/cm^2 and a normalized amplitude $a_0 = 1.11$. The wakefield is therefore resonantly excited by the laser train (see Fig. 3), and reaches the peak value of $\max(E_z) \simeq 0.9E_0$ in the bucket containing the bunch (see Fig. 5). Simulation of the laser-plasma (including ionization) process have been performed with the 2D-cylindrical hybrid QFluid code [50], including cross checks with ALaDyn code in the hybrid plasma configuration (fluid plasma background with kinetic trapped particles) and in the laser-envelope approximation [51–53].

Once we assured that the plasma wake's amplitude is in the optimal range for trapping the newborn electrons, the ionization pulse must be properly shaped and delayed with respect to the train. It is preferable that the ionization pulse is placed close to the node of the accelerating electric field and just after the fourth pulse in the high-intensity train. This maximizes both the amplitude of the plasma wave in the bucket where the newborn electrons are placed and the potential difference between the electric potential at the extraction point and at the injection point, thus promoting the trapping process itself. Having chosen Nitrogen as dopant, the ionizing pulse normalized amplitude $a_{0,\mathrm{ion}} = 0.63$ in the third harmonics of the Ti:Sa pulse and the amount of extracted charge (trapping efficiency is about 100%) of $Q = 30$ pC, an optimal minimum waist size of $w_{0,\mathrm{ion}} = 3.75$ μm should be obtained. Due to the passage of the ionizing pulse through the nonlinear crystal, an increase of 70% of the pulse duration has been assumed, together with a conversion efficiency of 15%. Therefore, to obtain an 80 mJ of pulse in third harmonics, a 500 mJ in fundamental harmonics is needed. This 17 TW laser pulse is obtained, from a fraction of the low-intensity stretched pulse, with a dedicate (small size) line consisting of an amplifier and a compressor. The third harmonics pulse should be tightly focused, so a (reflective) beam-expander enlarge it transversally so as to efficiently use a $F/1$ off-axis parabola (see Fig. 1(b), where the additional line for ReMPI is clearly visible). It is worth to note here that, being both the ionizing pulse and the driving train obtained from the same pulse (they share the same oscillator stage) the time jitter between them can arise from μm-size vibration solely, so it can be maintained within the (few of) femtosecond scale.

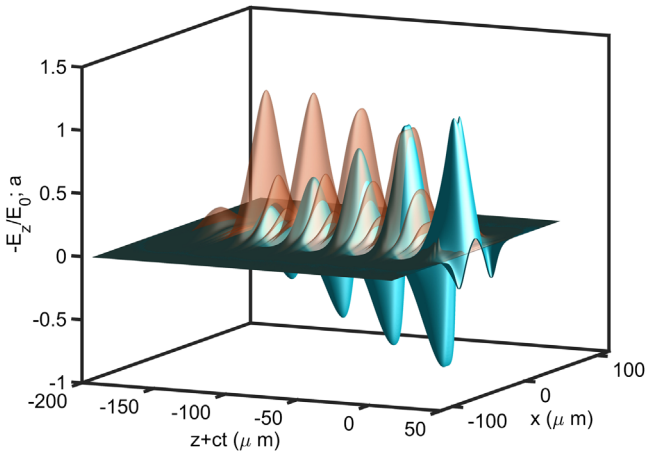

FIG. 3. $2D$ map of the longitudinal electric field E_z/E_0 with superimposed the map of the pulses train amplitude (transparent).

D. The quasiround beam option

The transverse phase space of the electrons extracted by field ionization of a single, linearly polarized pulse, is strongly asymmetric in the $x - p_x$ and $y - p_y$ planes, being electron quivering uniquely in the laser polarization axis. Therefore, as the beam evolves in the wakefield, an elliptical transverse shape is obtained soon. An high-density and elliptical bunch, however, do generate an asymmetric beam-loading effect that, in turn, triggers an asynchronous rotations in the $x - p_x$ and $y - p_y$ phase planes thus inducing a complex evolution of the transverse beam density profile. To avoid this, a (quasi) symmetric initial transverse phase space is necessary. In ReMPI this can be accomplished in two different ways.

In the simplest option a pulse of the train (polarized along y) and the x-polarized ionizing pulse do partially overlap (as in working point shown here). If the overlapping is not efficient, a further (low intensity) y-polarized pulse in the fundamental harmonics can be added so as to overlap the ionization pulse. In both cases, the amplitude of the y-polarized pulse a_y should be a small fraction of the ionization pulse amplitude, as we show in the following.

As a general case, consider an ionizing pulse in the Nth harmonics with amplitude a_i and the second pulse in the fundamental harmonics with amplitude a_s. The electric field from the pulses acting on an electron of the dopant is

$$E_{\mathrm{total}} = E_{0,l}\sqrt{N^2 a_i^2 \cos^2(\xi) + a_s^2 \cos^2(\xi/N + \phi)}, \quad (3)$$

where $E_{0,l} \equiv mc\omega_0/e$ is the reference laser field, $\xi = Nk_0(z_e + ct)$, is the particle phase in the ionizing pulse, z_e is the electron position and the phase shift ϕ refers to the phase difference between the two pulses. In the following we will suppose that $\epsilon \equiv a_s/(Na_i) \ll 1$.

For each ionizing pulse period, tunneling field ionization is efficient in a tiny slab in the vicinity of the electric field peak. Therefore, since the x and y components of the laser fields have an (almost) random phase correlation, after a 2nd order expansion of Eq. (3) in ϵ and some straightforward computation we get an estimate of the *rms* transverse momenta

$$\sigma(p_x/mc) \simeq \Delta^* a_i, \tag{4}$$

$$\sigma(p_y/mc) \simeq \frac{a_s}{\sqrt{2}}. \tag{5}$$

In Eq. (5), $\Delta^* = (1+\epsilon^2/4)\Delta$, where Δ is taken as in Ref. [45] and the correction is caused by the superposition of the y-polarized pulse. Equation (5) are strictly valid in the case $\Delta \ll 1$ and $N \gg 1$, so in our third harmonics working point with $N = 3$ and $\Delta = 0.3$ we expect some deviation of the theory from full-PIC simulation results. Nonetheless, the analytical estimation of the transverse phase-space shape is consistent with PIC simulations obtained with the FB-PIC code [54]. In Fig. 4 the analytical results of Eq. (5) for increasing values of a_s are shown, along with PIC simulation results. As a result, both analytical and numerical results agree in suggesting that a quasiround beam is obtained when $a_s \simeq \sqrt{2}\Delta^* a_i$, which means $\epsilon \simeq \Delta^*/N \ll 1$.

E. Simulation output up to plateau end

The target consists of a plasma obtained with a gas-jet delivering Nitrogen. Both the ionizing pulse and the driving train have been focused at the end of the up-ramp and the background plasma density profile, obtained supposing a pre-ionization of Nitrogen up to the fifth level, consists of a standard up-ramp of scale-length $L_{\rm up} = 800$ μm, a plateau of length $L_{\rm plateau} = 2.1$ mm with background density $n_e = 1.13 \times 10^{18}$ cm^{-3}, and a down-ramp of scale $L_{\rm down} = L_{\rm up}$.

The QFluid simulations assume a 2D *cylindrical* symmetry of the fields, while particles of the bunch move in a full-3D space. The bunch is sampled with $N_b = 1.06 \times 10^6$ equal-weighted macroparticles and the simulation box (a cylinder, actually) has radius 115 μm and length 210 μm. QFluid is equipped with a mesh-refining technique, which is activated in the longitudinal portion of the cylinder where the bunch is placed. The fields are solved in the quasistatic approximation [55] by using the coarse resolution of $dz_{\rm coarse} = 0.19$ μm (longitudinal) and $dr_{\rm coarse} = 0.38$ μm (radial), while the refined grid spacing are $dz_{\rm fine} = 0.05$ μm and $dr_{\rm fine} = 0.15$ μm.

During the charging phase, i.e., when the ionizing pulse electric field is large enough to extract the 6th electrons from N^{5+}, background density is approaching the plateau value, the maximum accelerating field is close to E_0 (see Fig. 5) and newborn electrons are being trapped in vicinity of the accelerating peak. A partial overlapping between the fourth high-intensity pulse of the train and the ionizing pulse successfully helped in generating a (quasi) round beam with very close x and y *rms* sizes and emittances (see Fig. 7). After trapping, a longitudinal phase-space rotation occurs (see Fig. 6) and at the end of the plateau the minimum energy spread is of about 1.6% with a mean

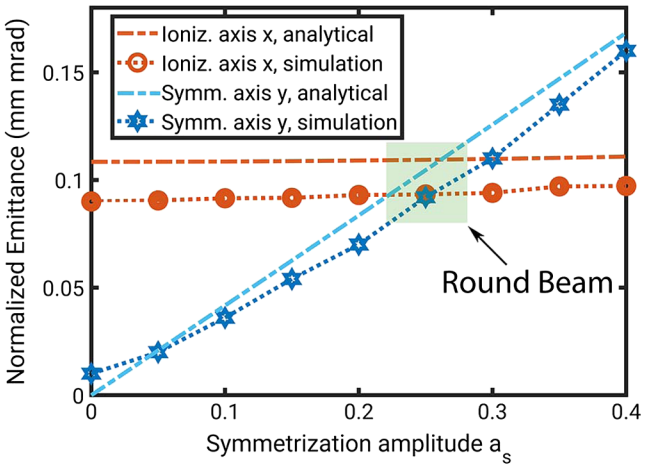

FIG. 4. Analytical results from Eq. (5) and PIC simulations obtained with FB-PIC of the electron beam emittances along the x (ionization pules polarization) and y (symmetrizing pulse) polarization axes. The ionization pulse has normalized amplitude $a_i = 0.63$, $N = 3$ (third harmonics), and is focused with a minimum waist $w_{0,\rm ion} = 3$ μm. The ionization and symmetrization pulses have FWHM duration of 30 fs. Both the analytical and simulated curves show that a (quasi) round beam can be obtained, in this configuration, with $a_s \simeq 0.25$.

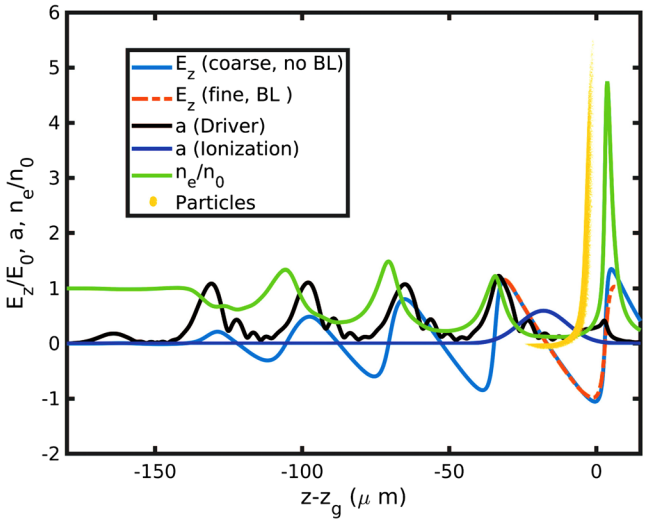

FIG. 5. Charging phase. On-axis lineout of the longitudinal electric field E_z without beam-loading (blue), of E_z in the refined grid and including beam-loading (dashed orange), of the plasma density (green), of the driving train amplitude (black) and of the third-harmonics ionizing pulse amplitude (purple). The longitudinal phase-space plot of the newborn electrons (yellow dots) is also visible.

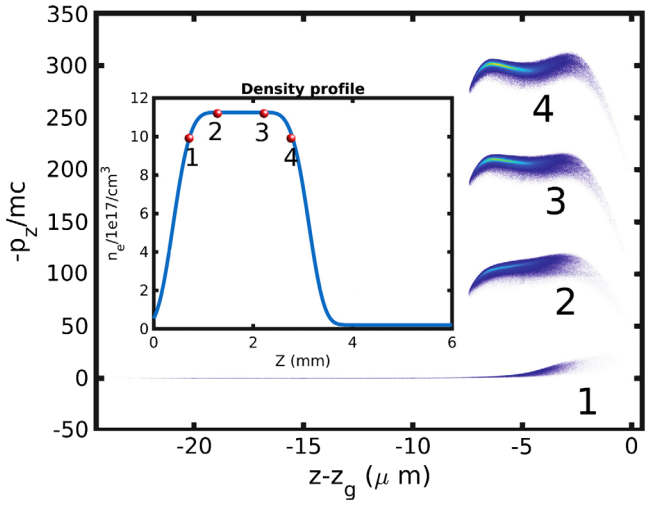

FIG. 6. Sequence of longitudinal phase-space densities in four distinct interaction points. Inset: background plasma density profile and position of the snapshot.

energy of 150 MeV and a total charge of $Q = 32$ pC. The transverse dynamics of the electron beam strongly depends on the time passed from its extraction from the ion. Within one (third harmonics) laser cycle from the extraction time, electrons start to quiver and got a residual transverse momentum after the interaction with the ionization pulse and (if the superposition occurs) the queue of the pulse in the train. Therefore, in addition to the estimate of the transverse momentum via Eqs. (1), (5), the transverse momentum acquired through transverse ponderomotive forces should be taken into account. Though the ponderomotive forces are in good approximation linear in the transverse coordinate and consequently do not contribute to the transverse emittance (see [45]), an indirect increase of normalized emittance due to ponderomotive forces occurs.

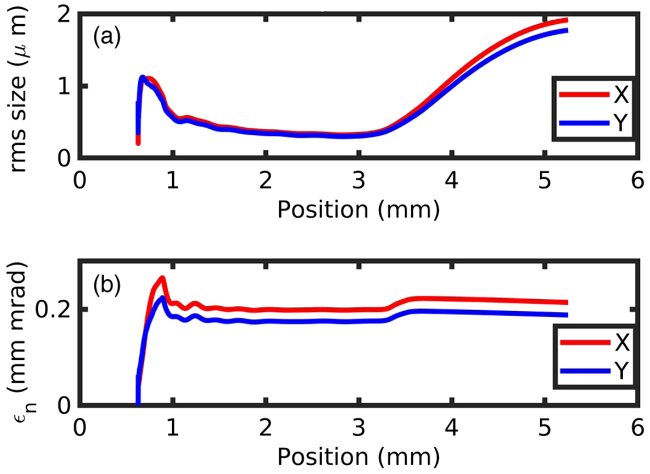

FIG. 7. a) Evolution of the *rms* bunch size in the x-direction (ionizing pulse polarization direction) and in the y-direction (driving train polarization direction). b) Evolution of the normalized emittances along x and y.

This is because the transverse kick on the low-energy electrons increases the beam radius just after the pulse passage and causes a fraction of the beam lying in a region of nonlinear transverse force. Those electrons, therefore, will oscillate with a lower betatron frequency, thus partially spoiling transverse quality. As bunch charge increases, space-charge and beam-loading can contribute to increase the beam emittance.

As a final result, phase mixing [56] and beam-charge induced nonlinearities can considerably reduce transverse beam quality. In our simulations the charging phase lasts for about $L_c \simeq 2Z_{R,\mathrm{ion}} = 2\pi w_{0,\mathrm{ion}}^2/\lambda_{\mathrm{ion}} = 330$ μm. During this phase (see Fig. 7) emittance initially increases and reaches a maximum at (roughly) 2/3 of the charging time, i.e., at position $z_g = \int \beta_g c dt \simeq 800$ μm in the graph. In the last portion of the charging phase normalized emittance reduces down the values of $\epsilon_{n,x} = 210$ nmrad and of $\epsilon_{n,y} = 230$ nmrad. This is caused by partial rephasing of the transverse phase-space ellipses [56]. As the beam remains matched during the whole acceleration phase, normalized emittance does not increase up to the bunch experiences varying transverse forces in the downramp (starting at $z_g \simeq 3$ mm in Fig. 7). We will discuss about the effect of the plasma lens in the following subsection. At the end of the acceleration phase, i.e., in the downramp region, the electron bunch has good quality except for the large divergence that would cause emittance degradation in the free space between the plasma and the first focusing element of the transport line. The use of a passive plasma lens helps us to considerably reduce the transverse momentum.

F. The downramp and the passive plasma lens

At the end of the plateau *rms* transverse momentum is $p_{x,y} \simeq 0.65\ mc$, with a resulting beam divergence $\sigma_\theta \simeq 3$ mrad and a very large Twiss parameter $\gamma \approx 6000$ m^{-1}. However, when γ is large, the emittance growth in the ballistic region scales as γ^2. Therefore, the mixing of the transverse phase space due to chromaticity effects would spoil out beam-quality soon out the plasma [27,28]. Decreasing γ at the plasma exit enables a dramatic reduction of the emittance growth in the transfer line downstream. It is known [57] that a smooth downramp can generate a transverse phase-space rotation, thus helping in reducing beam divergence. In the case of any MP-LWFA, however, the resonance condition is lost soon as density decreased during the downramp region and the matched smooth downramp profile condition in [57] cannot be satisfied. As a consequence, even in a long scale downramp (as in our simulated conditions) beam divergence got a reduction of just a 30% after the downramp (see Fig. 8).

To further reduce divergence, a passive plasma lens made by an Helium filled gas-cell, has been placed close to the

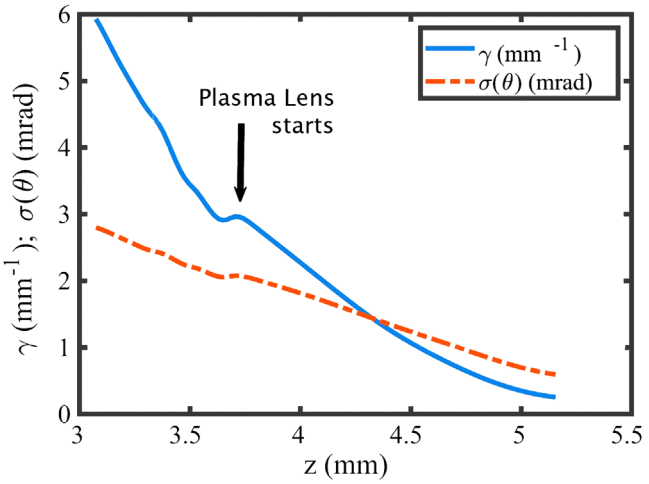

FIG. 8. Evolution of the Twiss γ parameter (blue line) and of the beam divergence (dashed orange line), starting from the end of the plateau. Plasma lens starts approximately at $z = 3.7$ mm. The minimum Twiss γ parameter is $\gamma = 0.14$ mm^{-1}.

gas-jet nozzle. The background plasma density of $n_{e,PL} = 1.0 \times 10^{16}$ cm^{-3} has been tuned so as to introduce a minimum increase of energy spread via beam-loading, though inducing an effective rotation of the transverse phase-space in a few mm scale length. As a result, after about 2.3 mm of propagation into the plasma lens, a phase-space rotation occurs without sizable increase of the normalized emittance (see Figs. 7 and 9) and a further reduction of about 60% of beam divergence from the end of the downramp. As a whole, the downramp and the plasma lens induced a reduction of about 80% of the beam divergence, while the Twiss γ parameter reduced to the acceptable value of $\gamma = 140$ m^{-1} starting from the very large initial value of about 6000 m^{-1}.

III. WORKING POINT STABILITY STUDY

Beam quality stability study involved tolerance analysis on pointing stability, driver-to-ionization pulses time jitter,

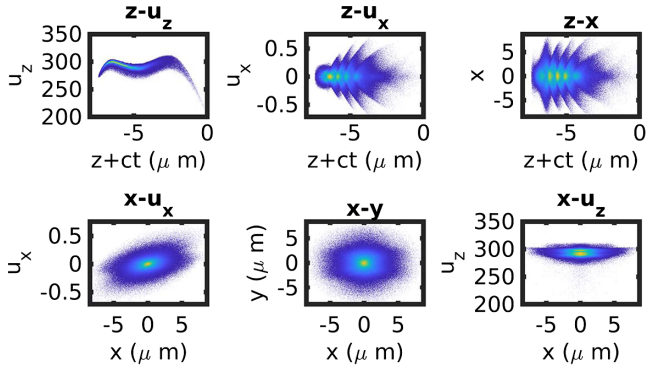

FIG. 9. Final bunch phase-space cuts. Longitudinal coordinate is $z + ct$ (laser and pulses move through negative z), $u_{x,y} = p_{x,y}/mc$ and $u_z = -p_z/mc$.

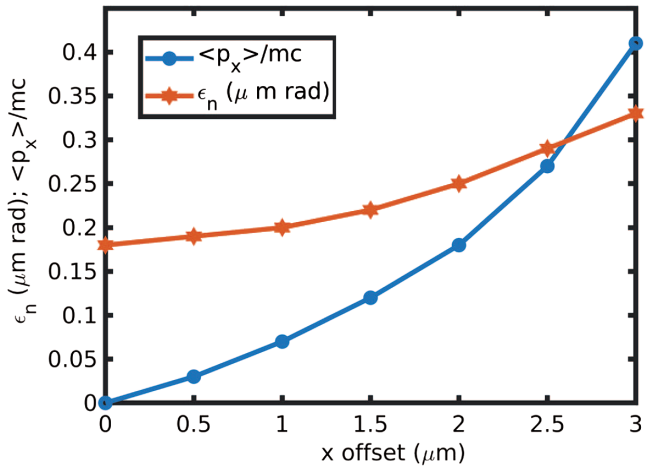

FIG. 10. Transverse jitter analysis. ALaDyn 2D slab simulations with varying transverse offset from the ionizing pulse (on axis) and the driving train. The x_{offset} represents the distance of the train center-of-mass from the simulation axis. The center-of-mass transverse momentum (orange) and the normalized emittance (blue) dependence on x_{offset} are shown.

pulses energies and background density fluctuations. Being QFluid a 2D code in *cylindrical* approximations for the fields, pointing stability analysis has been performed with the PIC code ALaDyn in 2D slab. Mechanical vibrations are expected to generate angular fluctuations in the pulses directions of μm rad scale. Having the driving train focusing parabola a focal length of about 2 m, the train of pulse is the most sensitive to pointing stability, while the ionization pulse transverse jitter at the interaction point is negligible. Electrons, therefore, at the leading order are extracted in the vicinity of the nominal axis but can experience transverse forces with a zero-axis placed at some distance (at most a few microns with our parameters) from the beam. As a consequence, a *mean* transverse momentum is gradually acquired as the beam evolves in the off-axis focusing force. The beam final transverse position $\langle x \rangle$, transverse momentum $\langle p_x \rangle$, as well as emittance, energy, and energy spread have been monitored in a set of ALaDyn simulations with different transverse offset of the driving train. Results clearly show that within a transverse jitter of 3 μm, bunch mean energy and energy spread are insensitive to pointing jitter (not shown here), while emittance and momentum center-of-mass show a quadratic dependence on the transverse offset (see Fig. 10).

The sensitivity of bunch parameters on plasma density and pulse energy fluctuations is basically linked to the dependence of the plasma wave amplitude and *phase* on the density and on the intensity of the pulses. In a MP-LWFA scheme the resonant excitation of the wake critically depends on the plasma wave that, therefore, must be fine-tuned in a reproducible fashion. With the parameters we found, from QFluid simulations, that to limit the bunch energy spread down to 2% *rms*, overall background density

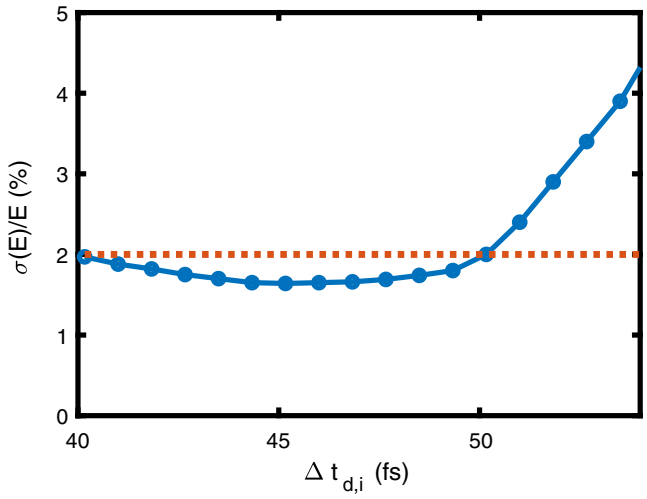

FIG. 11. Longitudinal jitter analysis. ALaDyn 2D slab simulations with varying transverse offset from the ionizing pulse (on axis) and the driving train. The x_{offset} represents the distance of the train center-of-mass from the simulation axis. The center-of-mass transverse momentum (orange) and the normalized emittance (blue) dependence on x_{offset} are shown.

fluctuation must be limited to 1.5% while driving train energy should be stabilized at 1.0% (FWHM) level.

The most critical parameter for bunch quality is timing jitter between the pulse train and the ionizing pulse. The train to ionizing pulse delay $\Delta d_{t,i}$ controls the phase of the extraction point in the plasma wave. Therefore, the trapping process critically depend on $\Delta d_{t,i}$ and thus the initial phase-space shape does. While normalized emittance is almost stable within our jitter scan of 15 fs, energy spread shows a diverging behavior, thus making the criticality of this parameter apparent. As we can infer in Fig. 11, however, if time jitter excursion is limited to 10 fs, an upper limit energy spread of 2% *rms* is obtained.

IV. CONCLUSIONS

In this paper we reported on simulations showing high-quality and high-current 150 MeV electron bunches production in a LWFA injector beamline based on the ReMPI scheme. We developed analytical results on the field-ionization process in presence of two, perpendicularly polarized, laser pulses with different wavelengths. Those results are confirmed by PIC simulations and helped us in generating a quasiround beam that has a beneficial impact on beam-loading control and beam transport.

This work is part of a design activity for the 150 MeV injector of the two-stages 5 GeV full-LWFA beamline in EuPRAXIA. Due to beam quality degradation in the ballistic region just after the injector, in the subsequent focusing beam optics and in the 5 GeV LWFA booster, a very demanding set of acceptable beam parameters at injector exit has been defined. This includes a charge $Q > 30$ pC, an energy spread $\sigma_E/E \ll 5\%$ and a very low emittance $\epsilon_n \ll 1$ μm rad. Since the bunch had to comply with all the constrains at once, the flexible and stable low-emittance ReMPI injection scheme has been selected. In ReMPI the optimal number of pulses in the driver train depends on the chosen dopant employed for the field-ionization of the newborn electron. We showed that the optimal dopant species depends on the maximum acceptable value of the normalized emittance. In order to comply with reliability criteria, we selected Nitrogen as a dopant. As a consequence, a relatively low number of four pulses in the train has been defined, which are able to excite a large amplitude plasma wave with $E_z/E_0 \simeq 0.9$.

The plasma target was a standard 2 mm long gas jet delivering Nitrogen, with a plasma background of about 10^{18} cm^{-3} obtained with a ionization up to the 5th level. During the electrons extraction and trapping phase, which occurred just before the up-ramp ended, electrons slept back in the plasma bucket and reached the plasma wave velocity just after the accelerating gradient peak, thus realizing the "strong trapping" process. As the propagation in the plateau proceeded, a longitudinal phase-space rotation occurred up to the plateau ended. Remarkably, in the plateau the normalized emittance did not increase, while a 10% increase of ϵ_n is observed at the end of the plasma downramp, where the Twiss γ has still the (very) large value of $\gamma \simeq 4000$ m^{-1}.

As we mentioned above, a beam with a large Twiss γ at plasma exit will experience a transverse quality degradation, soon in the ballistic region prior the transfer line entrance. To further reduce Twiss γ by more than one order of magnitude, a passive plasma lens is placed just after the down-ramp end. This is accomplished by inserting an Helium filled gas-cell, with plasma density $n_e = 10^{16}$ cm^{-3} and length of 2.5 mm. After the plasma lens exit, a manageable round beam with Twiss $\gamma = 140$ m^{-1}, energy spread of 1.65% and emittance 0.23 μmrad is finally obtained.

Furthermore, the stability study on the relevant parameters fluctuations revealed that the selected working point is stable against laser pulse energy and plasma background fluctuations, provided that reasonable upper limits of 1% for the latter and 1.5% (FWHM) for the former are satisfied. Moreover, a systematic scan of transverse jitter showed that within a few μm misalignments a negligible energy spread and emittance increase occurs. Yet, a parabolic dependence of the mean transverse momentum on the transverse jitter is found, thus helping in the design of the subsequent beam optics transfer line. We found, finally, that beam-quality is mostly sensitive to the longitudinal driver-to-ionization pulse jitter. Both the train and the ionization pulse, however, are obtained from the same low-energy pulse from the Ti:Sa oscillator. Therefore, the time jitter between them, of the order of a few femtoseconds, is mostly generated by mechanical vibrations and does not suffer of the typical issues emerging when pulses obtained with different laser systems are synchronized.

ACKNOWLEDGMENTS

The research leading to these results has received funding from the EU Horizon 2020 Research and Innovation Program under Grant Agreement No. 653782 EuPRAXIA. This project has received financial support from the CNR funded Italian research Network ELI-Italy. We acknowledge the S. Sinigardi grant IsB18_ALaRe and the P. Londrillo grant IsC65_ENV-LWFA at CINECA under the ISCRA initiative for the HPC resources. The authors very much appreciate the support by P. Londrillo (INAF, Italy) and M.Kirchen (DESY, Deutschland) for their help with ALaDyn and FB-PIC codes.

[1] O. Lundh, J. Lim, C. Rechatin, L. Ammoura, A. Ben-Ismaïl, X. Davoine, G. Gallot, J.-P. Goddet, E. Lefebvre, V. Malka *et al.*, Few femtosecond, few kiloampere electron bunch produced by a laser–plasma accelerator, Nat. Phys. **7**, 219 (2011).

[2] V. Petrillo, M. P. Anania, M. Artioli, A. Bacci, M. Bellaveglia, E. Chiadroni, A. Cianchi, F. Ciocci, G. Dattoli, D. Di Giovenale *et al.*, Observation of Time-Domain Modulation of Free-Electron-Laser Pulses by Multipeaked Electron-Energy Spectrum, Phys. Rev. Lett. **111**, 114802 (2013).

[3] A. Loulergue, M. Labat, C. Evain, C. Benabderrahmane, V. Malka, and M. E. Couprie, Beam manipulation for compact laser wakefield accelerator based free-electron lasers, New J. Phys. **17**, 023028 (2015).

[4] E. Esarey, S. K. Ride, and P. Sprangle, Nonlinear Thomson scattering of intense laser pulses from beams and plasmas, Phys. Rev. E **48**, 3003 (1993).

[5] P. Tomassini, A. Giulietti, D. Giulietti, and L. A. Gizzi, Thomson backscattering x-rays from ultra-relativistic electron bunches and temporally shaped laser pulses, Appl. Phys. B **80**, 419 (2005).

[6] S. Corde, K. Ta. Phuoc, G. Lambert, R. Fitour, V. Malka, A. Rousse, A. Beck, and E. Lefebvre, Femtosecond x rays from laser-plasma accelerators, Rev. Mod. Phys. **85**, 1 (2013).

[7] D. Micieli, I. Drebot, A. Bacci, E. Milotti, V. Petrillo, M. Rossetti Conti, A. R. Rossi, E. Tassi, and L. Serafini, Compton sources for the observation of elastic photon-photon scattering events, Phys. Rev. Accel. Beams **19**, 093401 (2016).

[8] S. Chen, N. D. Powers, I. Ghebregziabher, C. M. Maharjan, C. Liu, G. Golovin, S. Banerjee, J. Zhang, N. Cunningham, A. Moorti *et al.*, Mev-Energy X-rays from Inverse Compton Scattering with Laser-Wakefield Accelerated Electrons, Phys. Rev. Lett. **110**, 155003 (2013).

[9] K. T. Phuoc, S. Corde, C. Thaury, V. Malka, A. Tafzi, J.-P. Goddet, R. Shah, S. Sebban, and A. Rousse, All-optical compton gamma-ray source, Nat. Photonics **6**, 308 (2012).

[10] H.-E. Tsai, X. Wang, J. M. Shaw, Z. Li, A. V. Arefiev, X. Zhang, R. Zgadzaj, W. Henderson, V. Khudik, G. Shvets *et al.*, Compact tunable compton x-ray source from laser-plasma accelerator and plasma mirror, Phys. Plasmas **22**, 023106 (2015).

[11] B. Schroeder, E. Esarey, C. G. R. Geddes, C. Toth, and W. P. Leemans, *Advanced Accelerator Concepts*, edited by C. B. Schroeder, E. Esarey, and W. Leemans (AIP, NewYork, 2009), Vol. 1086, pp. 208–214.

[12] C. B. Schroeder, E. Esarey, C. G. R. Geddes, C. Benedetti, and W. P. Leemans, Physics considerations for laser-plasma linear colliders, Phys. Rev. Accel. Beams **13**, 101301 (2010).

[13] P. Muggli and B. C. Alegro, The advanced linear collider study group, in *9th Int. Particle Accelerator Conf.(IPAC'18), Vancouver, BC, Canada, April 29-May 4, 2018* (JACOW Publishing, Geneva, Switzerland, 2018), pp. 1619–1621.

[14] A. J. Gonsalves, K. Nakamura, J. Daniels, C. Benedetti, C. Pieronek, T. C. H. de Raadt, S. Steinke, J. H. Bin, S. S. Bulanov, J. van Tilborg *et al.*, Petawatt Laser Guiding and Electron Beam Acceleration to 8 Gev in a Laser-Heated Capillary Discharge Waveguide, Phys. Rev. Lett. **122**, 084801 (2019).

[15] A. Döpp, E. Guillaume, C. Thaury, A. Lifschitz, K. Ta Phuoc, and V. Malka, Energy boost in laser wakefield accelerators using sharp density transitions, Phys. Plasmas **23**, 056702 (2016).

[16] S. Steinke, J. Van Tilborg, C. Benedetti, C. G. R. Geddes, J. Daniels, K. K. Swanson, A. J. Gonsalves, K. Nakamura, B. H. Shaw, C. B. Schroeder *et al.*, Staging of laser-plasma accelerators, Phys. Plasmas **23**, 056705 (2016).

[17] T. L. Audet, F. G. Desforges, A. Maitrallain, S. D. Dufrénoy, M. Bougeard, G. Maynard, P. Lee, M. Hansson, B. Aurand, A. Persson *et al.*, Electron injector for compact staged high energy accelerator, Nucl. Instrum. Methods Phys. Res., Sect. A **829**, 304 (2016).

[18] G. Golovin, S. Banerjee, S. Chen, N. Powers, C. Liu, W. Yan, J. Zhang, P. Zhang, B. Zhao, and D. Umstadter, Control and optimization of a staged laser-wakefield accelerator, Nucl. Instrum. Methods Phys. Res., Sect. A **830**, 375 (2016).

[19] Z. Zhang, W. Li, J. Liu, W. Wang, C. Yu, Y. Tian, K. Nakajima, A. Deng, R. Qi, C. Wang *et al.*, Energy spread minimization in a cascaded laser wakefield accelerator via velocity bunching, Phys. Plasmas **23**, 053106 (2016).

[20] J. Faure, D. Gustas, D. Guénot, A. Vernier, F. Böhle, M. Ouillé, S. Haessler, R. Lopez-Martens, and A. Lifschitz, A review of recent progress on laser-plasma acceleration at khz repetition rate, Plasma Phys. Controlled Fusion **61**, 014012 (2018).

[21] P. A. Walker, P. D. Alesini, A. S. Alexandrova, M. P. Anania, N. E. Andreev, I. Andriyash, A. Aschikhin, R. W. Assmann, T. Audet, A. Bacci *et al.*, Horizon 2020 eupraxia design study, J. Phys. Conf. Ser. **874**, 012029 (2017).

[22] P. Tomassini, S. De Nicola, L. Labate, P. Londrillo, R. Fedele, D. Terzani, and L. A. Gizzi, The resonant multi-pulse ionization injection, Phys. Plasmas **24**, 103120 (2017).

[23] X. Li, P. A. P. Nghiem, and A. Mosnier, Toward low energy spread in plasma accelerators in quasilinear regime, Phys. Rev. Accel. Beams **21**, 111301 (2018).

[24] A. He, L. Yang, and L. Yu, *High-Gain Free-Electron Laser Theory, Introduction* (Springer International Publishing, Cham, 2014), pp. 1–37, ISBN 978-3-319-04507-8, https://doi.org/10.1007/978-3-319-04507-8_2-2.

[25] K. Floettmann, Adiabatic matching section for plasma accelerated beams, Phys. Rev. Accel. Beams **17**, 054402 (2014).

[26] X. L. Xu, J. F. Hua, Y. P. Wu, C. J. Zhang, F. Li, Y. Wan, C.-H. Pai, W. Lu, W. An, P. Yu *et al.*, Physics of Phase Space Matching for Staging Plasma and Traditional Accelerator Components using Longitudinally Tailored Plasma Profiles, Phys. Rev. Lett. **116**, 124801 (2016).

[27] M. Migliorati, A. Bacci, C. Benedetti, E. Chiadroni, M. Ferrario, A. Mostacci, L. Palumbo, A. R. Rossi, L. Serafini, and P. Antici, Intrinsic normalized emittance growth in laser-driven electron accelerators, Phys. Rev. Accel. Beams **16**, 011302 (2013).

[28] X. Li, A. Chancé, and P. A. P. Nghiem, Preserving emittance by matching out and matching in plasma wakefield acceleration stage, Phys. Rev. Accel. Beams **22**, 021304 (2019).

[29] S. Bulanov, N. Naumova, F. Pegoraro, and J. Sakai, Particle injection into the wave acceleration phase due to nonlinear wake wave breaking, Phys. Rev. E **58**, R5257 (1998).

[30] H. Suk, N. Barov, J. B. Rosenzweig, and E. Esarey, Plasma electron trapping and acceleration in a plasma wake field using a density transition, in *The Physics Of High Brightness Beams* (World Scientific, Singapore, 2000), pp. 404–417.

[31] P. Tomassini, M. Galimberti, A. Giulietti, D. Giulietti, L. A. Gizzi, L. Labate, and F. Pegoraro, Production of high-quality electron beams in numerical experiments of laser wakefield acceleration with longitudinal wave breaking, Phys. Rev. Accel. Beams **6**, 121301 (2003).

[32] C. G. R. Geddes, E. Cormier-Michel, E. Esarey, K. Nakamura, G. R. Plateau, C. B. Schroeder, C. S. Toth, D. L. Bruhwiler, J. R. Cary, and W. P. Leemans, Plasma gradient controlled injection and postacceleration of high quality electron bunches, AIP Conf. Proc. **1086**, 12 (2009).

[33] A. Buck, J. Wenz, J. Xu, K. Khrennikov, K. Schmid, M. Heigoldt, J. M. Mikhailova, M. Geissler, B. Shen, F. Krausz *et al.*, Shock-Front Injector for High-Quality Laser-Plasma Acceleration, Phys. Rev. Lett. **110**, 185006 (2013).

[34] H.-E. Tsai, K. K. Swanson, S. K. Barber, R. Lehe, H.-S. Mao, D. E. Mittelberger, S. Steinke, K. Nakamura, J. van Tilborg, C. Schroeder *et al.*, Control of quasi-monoenergetic electron beams from laser-plasma accelerators with adjustable shock density profile, Phys. Plasmas **25**, 043107 (2018).

[35] X. L. Xu, F. Li, W. An, T. N. Dalichaouch, P. Yu, W. Lu, C. Joshi, and W. B. Mori, High quality electron bunch generation using a longitudinal density-tailored plasma-based accelerator in the three-dimensional blowout regime, Phys. Rev. Accel. Beams **20**, 111303 (2017).

[36] L.-L. Yu, E. Esarey, C. B. Schroeder, J.-L. Vay, C. Benedetti, C. G. R. Geddes, M. Chen, and W. P. Leemans, Two-Color Laser-Ionization Injection, Phys. Rev. Lett. **112**, 125001 (2014).

[37] P. Tomassini, L. Labate, P. Londrillo, R. Fedele, D. Terzani, and L. A. Gizzi, High quality electron bunch production for high brilliance thomson scattering sources, in *SPIE Optics + Optoelectronics* (International Society for Optics and Photonics, Prague, 2017), pp. 102400T–102400T, https://doi.org/10.1117/12.2266938.

[38] P. Tomassini, S. De Nicola, L. Labate, P. Londrillo, R. Fedele, D. Terzani, F. Nguyen, G. Vantaggiato, and L. A. Gizzi, High-quality gev-scale electron bunches with the resonant multi-pulse ionization injection, Nucl. Instrum. Methods Phys. Res., Sect. A **909**, 1 (2018).

[39] D. Umstadter, E. Esarey, and J. Kim, Nonlinear Plasma Waves Resonantly Driven by Optimized Laser Pulse Trains, Phys. Rev. Lett. **72**, 1224 (1994).

[40] S. M. Hooker, R. Bartolini, S. P. D. Mangles, A. Tünnermann, L. Corner, J. Limpert, A. Seryi, and R. Walczak, Multi-pulse laser wakefield acceleration: A new route to efficient, high-repetition-rate plasma accelerators and high flux radiation sources, J. Phys. B **47**, 234003 (2014).

[41] R. J. Shalloo, L. Corner, C. Arran, J. Cowley, G. Cheung, C. Thornton, R. Walczak, and S. M. Hooker, Generation of laser pulse trains for tests of multi-pulse laser wakefield acceleration, Nucl. Instrum. Methods Phys. Res., Sect. A **829**, 383 (2016).

[42] J. Cowley, C. Thornton, C. Arran, R. J. Shalloo, L. Corner, G. Cheung, C. D. Gregory, S. P. D. Mangles, N. H. Matlis, D. R. Symes *et al.*, Excitation and Control of Plasma Wakefields by Multiple Laser Pulses, Phys. Rev. Lett. **119**, 044802 (2017).

[43] M. Chen, Z.-M. Sheng, Y.-Y. Ma, and J. Zhang, Electron injection and trapping in a laser wakefield by field ionization to high-charge states of gases, J. Appl. Phys. **99**, 056109 (2006).

[44] F. Li, J. F. Hua, X. L. Xu, C. J. Zhang, L. X. Yan, Y. C. Du, W. H. Huang, H. B. Chen, C. X. Tang, W. Lu *et al.*, Generating High-Brightness Electron Beams via Ionization Injection by Transverse Colliding Lasers in a Plasma-Wakefield Accelerator, Phys. Rev. Lett. **111**, 015003 (2013).

[45] C. B. Schroeder, J.-L. Vay, E. Esarey, S. S. Bulanov, C. Benedetti, L.-L. Yu, M. Chen, C. G. R. Geddes, and W. P. Leemans, Thermal emittance from ionization-induced trapping in plasma accelerators, Phys. Rev. Accel. Beams **17**, 101301 (2014).

[46] C. W. Siders, J. L. W. Siders, A. J. Taylor, S.-G. Park, and A. M. Weiner, Efficient high-energy pulse-train generation using a 2 n-pulse Michelson interferometer, Appl. Opt. **37**, 5302 (1998).

[47] B. Dromey, M. Zepf, M. Landreman, K. O'keeffe, T. Robinson, and S. M. Hooker, Generation of a train of ultrashort pulses from a compact birefringent crystal array, Appl. Opt. **46**, 5142 (2007).

[48] L. A. Gizzi, P. Koester, L. Labate, F. Mathieu, Z. Mazzotta, G. Toci, and M. Vannini, A viable laser driver for a user plasma accelerator, Nucl. Instrum. Methods Phys. Res., Sect. A **909**, 58 (2018).

[49] O. Morice, Miró: complete modeling and software for pulse amplification and propagation in high-power laser systems, Opt. Eng. **42**, 1530 (2003).

[50] P. Tomassini and A. R. Rossi, Matching strategies for a plasma booster, Plasma Phys. Controlled Fusion **58**, 034001 (2016).

[51] D. Terzani and P. Londrillo, A fast and accurate numerical implementation of the envelope model for laser–plasma dynamics, Comput. Phys. Commun. **242**, 49 (2019).

[52] C. Benedetti, A. Sgattoni, G. Turchetti, and P. Londrillo, ALaDyn: A high-accuracy pic code for the Maxwell–Vlasov equations, IEEE Trans. Plasma Sci. **36**, 1790 (2008).

[53] S. Stefano, T. Davide, M. Alberto, L. Pasquale, M. Francesco, M. Francesco, and S. Andrea, Aladyn/aladyn: Aladyn v2019.1, April 2019. https://doi.org/10.5281/zenodo.2626679.

[54] R. Lehe, M. Kirchen, I. A. Andriyash, B. B. Godfrey, and J.-L. Vay, A spectral, quasi-cylindrical and dispersion-free particle-in-cell algorithm, Comput. Phys. Commun. **203**, 66 (2016).

[55] P. Sprangle, E. Esarey, and A. Ting, Nonlinear Theory of Intense Laser-Plasma Interactions, Phys. Rev. Lett. **64**, 2011 (1990).

[56] X. L. Xu, J. F. Hua, F. Li, C. J. Zhang, L. X. Yan, Y. C. Du, W. H. Huang, H. B. Chen, C. X. Tang, W. Lu *et al.*, Phase-Space Dynamics of Ionization Injection in Plasma-Based Accelerators, Phys. Rev. Lett. **112**, 035003 (2014).

[57] I. Dornmair, K. Floettmann, and A. R. Maier, Emittance conservation by tailored focusing profiles in a plasma accelerator, Phys. Rev. Accel. Beams **18**, 041302 (2015).